

Enhancement in thermal stability and surface properties of $\text{LiFePO}_4/\text{VFLG}$ composite prepared via sol-gel route

Amun Amri^{a,*}, Yola Bertilsya Hendri^a, Sunarno^a, Yoyok Dwi Setyo Pambudi^b, Mazhibayev Assylzhan^c, Kambarova Elmira^c, Khusnul Ain^d, Khairulazhar Jumbri^e, Zhong Tao Jiang^f, Chun-Chen Yang^g

^aDepartment of Chemical Engineering, University of Riau, Pekanbaru 28293, Indonesia

^bResearch Center for Nuclear Reactor Technology, BRIN, Tangerang Selatan 15314, Indonesia

^cDepartment of Chemistry, Taraz University named after M.Kh. Dulaty, Taraz 080000, Kazakhstan

^dDepartment of Biomedical Engineering, Universitas Airlangga, Surabaya 60115, Indonesia

^eDepartment of Fundamental and Applied Sciences, Universiti Teknologi PETRONAS, Seri Iskandar 32610, Malaysia

^fSurface Analysis and Materials Engineering Research Group, Murdoch University, WA 6150, Australia

^gBattery Research Center of Green Energy, Ming Chi University of Technology, Taishan, New Taipei City 24301, Taiwan

Article history:

Received: 26 February 2025 / Received in revised form: 9 May 2025 / Accepted: 10 May 2025

Abstract

Thermal and surface properties of $\text{LiFePO}_4/\text{very-few-layer graphene}$ ($\text{LiFePO}_4/\text{VFLG}$) composite manufactured through the sol-gel route have been researched for lithium-ion battery cathode application. VFLG was acquired from a facile, cost-effective, and environmentally benign fluid dynamic shear exfoliation process. The composites were characterized through thermogravimetry analysis (TGA), differential scanning calorimetry (DSC), field-emission scanning electron microscopy (FESEM) interlinked with energy-dispersive X-ray spectroscopy (EDX), transmission electron microscopy (TEM), high-resolution transmission electron microscopy (HRTEM), and Brunauer-Emmett-Teller (BET) analysis. The TGA-DSC results showed that the integration of VFLG could enhance the thermal stability of the composite by inhibiting oxygen diffusion on the LiFePO_4 surface. FESEM-EDX analysis, meanwhile, confirmed the homogeneously distributed VFLG in the composites. TEM results revealed that the average particle sizes of the composites decreased by about 21.2% compared to the bare LiFePO_4 . TEM and HRTEM results confirmed an intimate contact between VFLG intimately and LiFePO_4 particles via plane-to-point contact, contributing to the control and reduction of particle size. Furthermore, physisorption via BET analysis revealed that incorporating VFLG provided a wider distribution of mesopores and increased pore diameter and pore volume by 128.7% and 656.3%, respectively, compared to sole LiFePO_4 . These significant improvements were related to the flexibility and ability of a thin layer of VFLG to limit the growth of LiFePO_4 particles. This approach offers a promising strategy to enhance the thermal stability and surface properties of lithium-ion battery cathodes.

Keywords: Sol-gel route, $\text{LiFePO}_4/\text{VFLG}$ composite, thermal stability, surface properties, pore distribution

1. Introduction

Lithium iron phosphate (LiFePO_4), considering its long cycle life, high safety, and eco-friendliness, has emerged as a prospective cathode material for lithium-ion batteries (LIBs) [1,2]. Its lower electrical conductivity and thermal stability, however, still limit its widespread use, particularly in high-performance applications requiring these properties [3,4]. Various efforts have then been made to overcome these limitations by modifying its structure and composition [3,5]. Of the strategies investigated, the addition of carbon-based conductive materials has shown significant potential for the enhancement of these properties [6,7].

Integrating graphene is considered among the most effective ways to elevate the efficiency of LiFePO_4 [8,9]. Graphene, a carbon allotrope with exceptional electrical conductivity, a large surface area, and excellent thermal behavior [10,11], has become a popular additive to advance the electrochemical capabilities of LIB cathode materials. The integration of graphene can address the conductivity challenges of LiFePO_4 by creating a conductive network enabling to improve electron transport and overall battery efficiency [8]. The thermal stability of LiFePO_4 can also be enhanced by adding graphene, which serves as a thermal distributor, to decrease the risk of overheating and thermal runaway, which are the critical issues in battery applications [12].

The addition of graphene in the LiFePO_4 cathode has also been reported to significantly impact the morphology of the material, leading to the generation of numerous mesopores that

* Corresponding author. Tel.: (+62) 751- 72497; fax: (+62) 751 - 72566

Email: taufiqhsan@eng.unand.ac.id

<https://doi.org/10.21924/cst.10.1.2025.1667>



then create a unique 3D conductive network structure [13]. This unique structure later on results in a better rate and cyclic efficiency of the cathode due to its high conductivity and abundant mesopores, which accelerate the Li^+ ion transport [13]. An excessive graphene addition, nonetheless, can reduce the total energy density and performance; as a consequence, a careful control in adding the graphene amount is highly critical [14,15]. Furthermore, the structure and number of graphene layers also determine the morphology of LiFePO_4 [16]. Both single-layer and multilayer graphene can improve the morphology and electrochemical capabilities of LiFePO_4 . The excessive number of layers, however, can become a significant barrier to lithium-ion movement in which it can increase the ion transport path length, and ultimately reduce ionic conductivity [16]. The thinner the graphene layers, the more efficient the conductive network formed within the cathode material [17]. Typically, FLG (few-layer graphene) consists of 4-8 graphene layers [18, 19], while VFLG (very-few-layer graphene) is primarily composed of 1-3 graphene layers [20].

Chemical vapor deposition (CVD) that produces single-layer graphene can deliver superior LIB performance [21]. Nevertheless, the transfer process, its homogeneity within the cathode composite, and the high processing costs of CVD-derived graphene still limit its commercial feasibility [7]. Incorporating graphene oxide (GO) or reduced graphene oxide (rGO) to LiFePO_4 cathodes shows good dispersion and homogeneity, as well as excellent specific capacity [22], but defects in rGO can reduce charge carrier mobility and limit high-temperature stability [23]. Furthermore, the prolonged GO preparation process involving less environmentally friendly chemicals has reduced interest in the use of this material. Wang J. et al. [24] reported that few-layer graphene (FLG), obtained through a liquid-phase exfoliation method, could significantly enhance the electrochemical capabilities of LiFePO_4 cathodes, even at relatively low loadings (~ 3 wt%) [24]. However, the preparation of a cavitation jet system to form graphene flakes and powder (a two-step process) is cumbersome and involves the use of acetone, which is relatively less environmentally friendly [24]. Based on the above discussion, the use of thinner graphene can lead to a more efficient conductive network, thereby optimizing LiFePO_4 cathode performance.

The addition of very few-layers graphene (VFLG) to LiFePO_4 cathodes has attracted significant attention as a promising approach to enhance the cathode performance in relation to the minimal number of graphene layers, the facile and low-cost production process, and its environmentally friendly nature [20]. In our previous study, we successfully enhanced the electrochemical capabilities of LiFePO_4 cathodes after the addition of VFLG using the sol-gel method in which it resulted in improvements in the lattice parameter of LiFePO_4 , an improvement in specific discharge capacity reaching 58.3%. Cyclic voltammetry and electrochemical impedance spectroscopy exhibited that LFP/VFLG displayed minimal internal resistance, excellent electrochemical reaction reversibility, an elevated Li^+ diffusion coefficient, and minimal polarization [9]. This study explored the outcome of adding VFLG on the thermal behavior and morphology of LiFePO_4 cathodes. The direct integration of low-cost very few-layer graphene (VFLG) (obtained through a straightforward and

environmentally friendly liquid shear exfoliation process) into LiFePO_4 lithium-ion cathodes, offers a novel strategy to elevate the performance of LiFePO_4 lithium-ion cathodes. This method reduces both production costs and environmental impact. The investigation involved thermal analysis using TGA-DSC, morphological analysis via FESEM-EDX and TEM-HRTEM, as well as physisorption analysis through BET testing. The results indicated improvements in thermal properties and morphology after the addition of VFLG to LiFePO_4 in view of the flexibility and thin-layer structure of VFLG, which restricted particle growth within LiFePO_4 . In the context of LiFePO_4 as a cathode for lithium-ion batteries, the addition of VFLG provides more conductive sites, optimizing the electrochemical capabilities of LiFePO_4 as a LIB cathode.

2. Materials and Methods

2.1. Preparation of VFLG

VFLG was synthesized from natural graphite using facile two-step shear exfoliation in an aqueous solution [20]. The solution is derived from an affordable domestic dishwashing liquid comprising 18.9% sodium lauryl sulfate (SLS) as an active and stabilizing compound. In the first step, the solution is exfoliated through a turbulence-assisted shear exfoliation (TASE) process in a rotating blade mixer, and after 24 hours, the liquid is separated from the residue. In the second step, the resulting liquid was fed into the highly effective L5M high-shear mixer for 120 min to complete the exfoliation process. This process in the end produced the graphene solutions.

2.2. Preparation of LiFePO_4 and LiFePO_4 /VFLG composites

The synthesis of LiFePO_4 was carried out using lithium dihydrogen phosphate (LiH_2PO_4) (Sigma-Aldrich, St Louis, MO) and iron (III) citrate ($\text{C}_6\text{H}_5\text{FeO}_7$) (Sigma-Aldrich, $\geq 99.99\%$) as the base materials. The solutions of LiH_2PO_4 and $\text{C}_6\text{H}_5\text{FeO}_7$, both in equimolar proportions, were combined and heated to 60°C while stirring for 10 minutes with a heated magnetic stirrer. The solution was dehydrated at 70°C for 24 hours to produce a dense xerogel, which was later grinded in a mortar for around 20 min and calcined under an Argon atmosphere at 700°C for 10 hours. To prepare LiFePO_4 /VFLG composites, 8% wt VFLG liquid was added, and all the preparation methods followed the same thorough route [9].

2.3. Characterizations

LiFePO_4 and LiFePO_4 /VFLG composites were characterized through thermogravimetry (TGA) analysis, differential scanning calorimetry (DSC) analysis, field-emission scanning electron microscopy (FESEM) interlinked with Energy-dispersive X-ray spectroscopy (EDX), transmission electron microscopy (TEM), high-resolution transmission electron microscopy (HRTEM), and physisorption analysis. Here, TGA and DSC analysis were performed by means of a TGA/DSC 3+ High-temperature furnace, Mettler Toledo). FESEM analysis was performed using FEI Nova NanoSem 230 (FEI, Hillsboro, Oregon, USA) equipment

interlinked with EDX (EDX Max 20, Oxford Instrument, Oxford, UK). Furthermore, TEM was performed using a JEOL JEM 1400 Instrument (JEOL, Peabody, MA, USA) with a 120 kV voltage applied for acceleration, while HRTEM was processed using the JEOL JEM-2100F Field Emission TEM (JEOL JEM-2100F, JEOL Ltd., Tokyo, Japan), with a 200 kV accelerating voltage applied. For the physisorption analysis, the specific surface areas of LiFePO_4 products were assessed using the multi-point Braneur-Emmett-Teller (BET) technique, while the Barrett-Joyner-Halenda (BJH) pore size distribution was determined from the desorption segment of the isotherm with Quantachrome Instrument (Version 3.01).

3. Results and Discussion

3.1. TGA-DSC analysis

Fig. 1 and Fig. 2 present the diagram of the formation of $\text{LiFePO}_4/\text{VFLG}$ composites and the TGA-DSC curves of LiFePO_4 and $\text{LiFePO}_4/\text{VFLG}$ composites at a 10 K/min heating rate under airflow, respectively. As observed, the TGA-DSC curves for LiFePO_4 and $\text{LiFePO}_4/\text{VFLG}$ composites had an almost similar trend. The TGA curve of LiFePO_4 and $\text{LiFePO}_4/\text{VFLG}$ composites (Fig. 2(a)) showed a significant mass loss in the temperature range around 400°C - 550°C with the mass loss of LiFePO_4 and $\text{LiFePO}_4/\text{VFLG}$ composites by $\sim 6.8\%$ and $\sim 6.5\%$, respectively. This mass loss was related to an oxidation reaction of carbon and LiFePO_4 occurred at high temperatures, as seen in equation (1), as reported by Belharouak et al. [25].

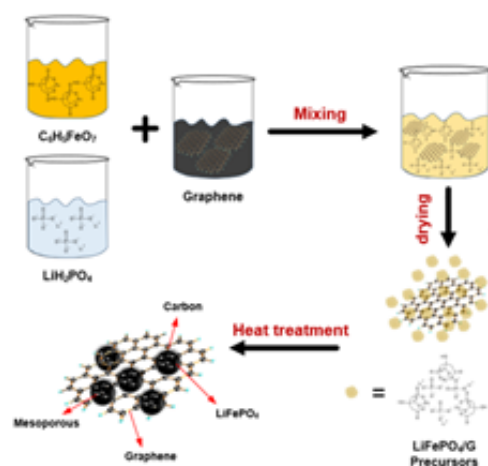
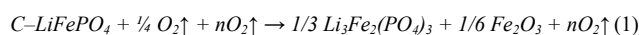


Fig. 1. The schematic of the formation of $\text{LiFePO}_4/\text{VFLG}$ composites

Fig. 2(a) shows that the $\text{LiFePO}_4/\text{VFLG}$ composite exhibited a mass loss lower than that of pure LiFePO_4 , suggesting that the incorporation of graphene could improve the thermal stability of the $\text{LiFePO}_4/\text{VFLG}$ composite. Graphene can shield the underlying substance from damage by reason of intense heat and distribute the thermal energy evenly to mitigate structural degradation [26]. This suggests that graphene can become a thermal barrier that is able to improve material resistance to degradation at high temperatures.

Fig. 2(b) illustrates the DSC curve of LiFePO_4 and

$\text{LiFePO}_4/\text{VFLG}$ composites. The exothermic peaks of LiFePO_4 and $\text{LiFePO}_4/\text{VFLG}$ composites were observed at 416.82°C and 417.43°C , respectively. The slight shift of the exothermic peak to a higher temperature in $\text{LiFePO}_4/\text{VFLG}$ composites indicated that the oxygen diffusion onto the LiFePO_4 surface was slightly inhibited by the VFLG layer, leading the oxidation temperature to slightly increase (0.15% increase) [27]. Nevertheless, as reported by Wei et al. [27] this layer will not retard lithium-ion diffusion in the charge/discharge process in LIB application [27]. The inhibition of oxygen diffusion at the LiFePO_4 surface may occur in view of several possibilities. First, at high temperatures, graphene is able to form strong covalent bonds with oxygen atoms on the LiFePO_4 surface. These bonds then reduce oxygen mobility on the surface, thereby inhibiting oxygen diffusion. A study showed that the strong C–O bonds on the surface of graphene made it more difficult for oxygen to move freely [28]. The second possibility is that oxygen molecules adsorbed on the graphene surface may trigger competition with other molecules, such as hydrogen or nitrogen, which can also be adsorbed on the same surface. This competition can then reduce the amount of oxygen interacting with the LiFePO_4 surface [29]. Thirdly, graphene may cover the active sites on the LiFePO_4 surface, commonly used for reactions with oxygen. By covering these sites, graphene reduces the amount of oxygen that can diffuse and react on the LiFePO_4 surface [30].

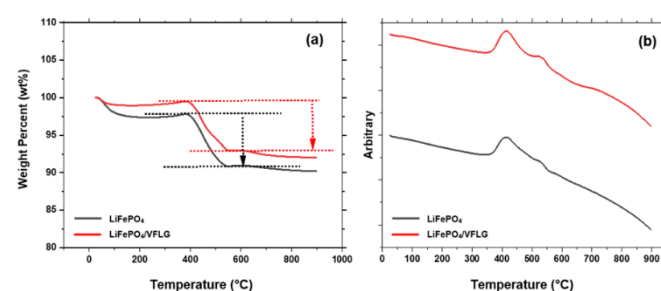


Fig. 2. (a) TGA curves of LiFePO_4 and $\text{LiFePO}_4/\text{VFLG}$, (b) DSC curves of LiFePO_4 and $\text{LiFePO}_4/\text{VFLG}$

3.2. FESEM-EDX analysis

Fig. 3 reveals the FESEM images of LiFePO_4 and $\text{LiFePO}_4/\text{VFLG}$ composites. Fig. 3 (a, b) shows that the $\text{LiFePO}_4/\text{VFLG}$ composites provided an homogeneous distribution of LiFePO_4 particles, likely due to the even dispersion of graphene in the LiFePO_4 precursor suspension [31], which prevents the aggregation of LiFePO_4 particles [32]. These findings are consistent with the report by Tian et al. [33] revealing that LiFePO_4 modified with graphene of high electrical conductivity displayed a uniform particle morphology. A close view showed the appearance of mesoporous structures in LiFePO_4 and $\text{LiFePO}_4/\text{VFLG}$ composites, as shown in Fig. 3 (c, d). It is worth noting that the porous structure in LiFePO_4 and $\text{LiFePO}_4/\text{VFLG}$ composites is determined by the evolved gases (water vapor (H_2O), carbon monoxide (CO), and carbon dioxide (CO_2)) during the dehydration process, as well as the decomposition of iron (III) citrate and lithium dihydrogen phosphate [34].

Fig. 3(d) shows the presence of graphene covering the

LiFePO₄ surface. As observed, graphene intimately contacted with LiFePO₄ particles by plane-to-point contact as graphene sheets have the outstanding flexibility and thin and high surface area [32]. Graphene sheets act as a conductive additive and support the LiFePO₄ structure, connecting separated or isolated LiFePO₄ particles to form a more effective conducting network [32]. The conducting network of graphene provides a fast pathway for electron migration during the charge/discharge process, improving electron conductivity in LIB applications [32].

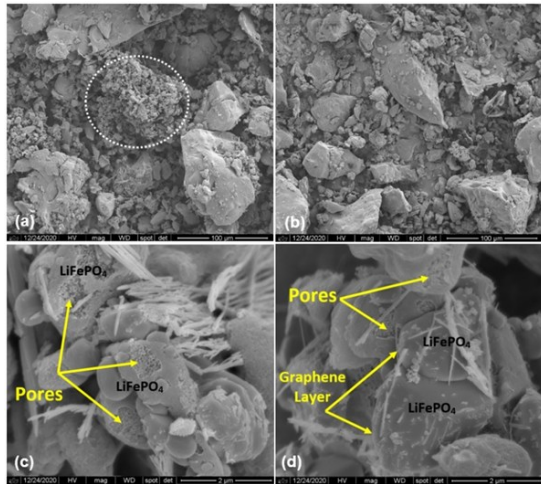


Fig. 3. FESEM image of (a) LiFePO₄ at scale bar of 100 μm, (b) LiFePO₄/VFLG at scale bar of 100 μm, (c) LiFePO₄ at scale bar of 2 μm, (d) LiFePO₄/VFLG at scale bar of 2 μm

Fig. 4 shows the EDX mapping of LiFePO₄/VFLG composites in which Fe, P, and O elements were uniformly distributed. In addition, C element appeared to be well distributed in all parts, indicating a homogeneous graphene distribution. Table 1 presents the percentages of iron (Fe), phosphorus (P), oxygen (O), and carbon (C) contained in LiFePO₄ and LiFePO₄/VFLG composites. The EDX results confirmed that graphene has been successfully incorporated into LiFePO₄, as proven by increased carbon composition. Moreover, both samples showed a Fe:P:O ratio close to 1:1:4, corresponding to the structure of LiFePO₄.

Table 1. Percentage of elements in LiFePO₄ and LiFePO₄/VFLG composites

Elements	LiFePO ₄		LiFePO ₄ /VFLG	
	Weight percentages (%wt.)	Atomic percentages (at. %)	Weight percentages (%wt.)	Atomic percentages (at. %)
C	20.57	35.08	22.22	38.12
O	34.14	43.70	31.14	40.10
P	15.67	10.36	15.45	10.28
Fe	29.62	10.86	31.19	11.50

3.3. TEM and HRTEM analysis

The presence of graphene was further identified using a TEM analysis. Fig. 5 displays the TEM images of LiFePO₄ and LiFePO₄/VFLG composites. It was found that the graphene

sheets were evenly distributed on the surface of the LiFePO₄ particles to form LiFePO₄/VFLG composites. The interactions between LiFePO₄ and graphene in LiFePO₄/VFLG composites have been studied by Wang et al. [35]. It has been reported that there is an interfacial binding between LiFePO₄ and graphene in a parallel orientation [35]. The interfacial binding energies (E_{bin}) per unit area of LiFePO₄/VFLG was reported as ~20.18 meV/Å² [35], where this value was within the Van der Waals binding energy interval (13-21 meV/Å²), indicating that the Van der Waals bond has a significant contribution in the interaction between LiFePO₄ and graphene [35].

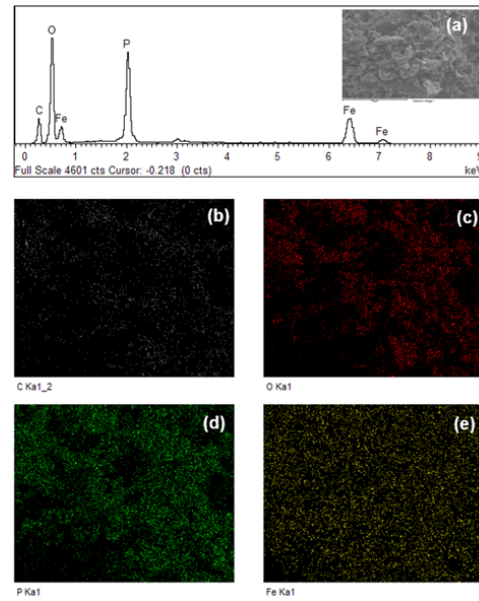


Fig. 4. (a) Energy spectrum of the elements in the sample, (b-e) EDX mapping of carbon, oxygen, phosphorus, and iron elements, respectively.

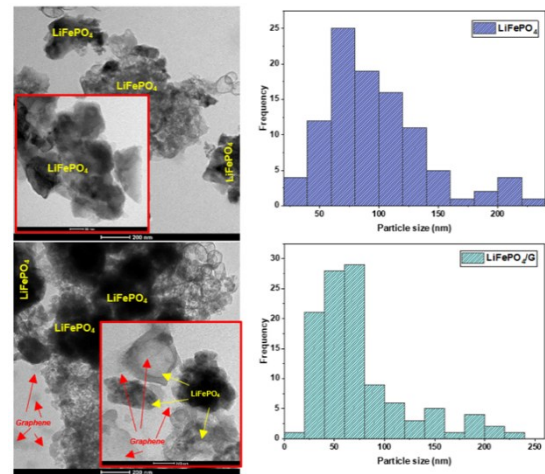


Fig. 5. TEM images of LiFePO₄ and LiFePO₄/VFLG

The mean particle sizes of LiFePO₄ and LiFePO₄/VFLG composites were 95.98 nm and 75.60 nm, respectively. These results indicated that incorporating graphene reduced the particle size of LiFePO₄. This can be explained by graphene acting as a separator, impeding the growth and agglomeration of LiFePO₄ particles [36]. Generally, smaller particle size will provide a sufficient contact area for LiFePO₄/electrolyte and shorten the Li⁺ diffusion pathway, leading to the enhancement of the electrochemical capabilities of the LIB cathode [33].

Fig. 6 illustrates HRTEM image of LiFePO_4 and $\text{LiFePO}_4/\text{VFLG}$ composites. It is observable that a thin layer of amorphous carbon coated both LiFePO_4 and $\text{LiFePO}_4/\text{VFLG}$ composites with a thickness of about $\sim 1\text{--}2\text{ nm}$, which originated from the citrate decomposition during the synthesis reaction (Fig. 6(a,d)). The inserts in Fig. 6 (a,d) showed a corresponding Fast Fourier-Transform (FFT) pattern, displaying a single crystal pattern with sharp diffraction points. Furthermore, Fig. 6(b,e) and 6(c,f) show the Fast inverse Fourier-Transform (Inverse-FFT) and line profile for inverse-FFT. Based on the line profile of inverse-FFT, d spacing values of LiFePO_4 and $\text{LiFePO}_4/\text{VFLG}$ composites were 0.39 nm and 0.391 nm , respectively, which corresponded to the orthorhombic (210) plane. Furthermore, the presence of graphene in LiFePO_4 is seen in Fig. 6(d), where graphene layers coated and connected LiFePO_4 particles to form an effective conducting network [32].

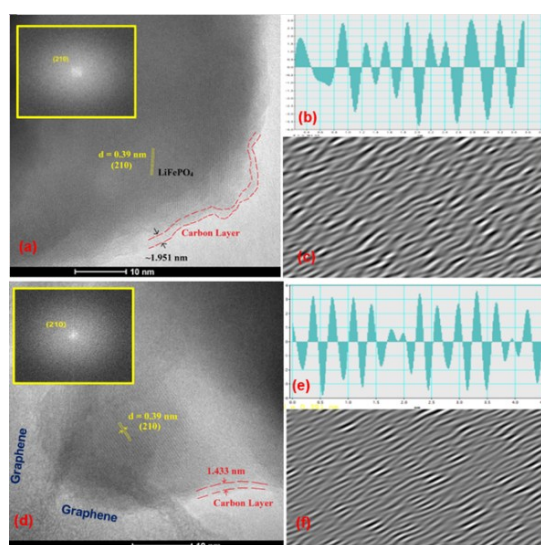


Fig. 6. (a) HRTEM image of LiFePO_4 , (b) Inverse FFT of LiFePO_4 , (c) FFT of LiFePO_4 , (d) HRTEM image of $\text{LiFePO}_4/\text{VFLG}$ composites, (e) Inverse-FFT of $\text{LiFePO}_4/\text{VFLG}$ composites, (f) FFT of $\text{LiFePO}_4/\text{VFLG}$ composites

3.4. BET analysis

To investigate the surface characteristics of LiFePO_4 and $\text{LiFePO}_4/\text{VFLG}$ composites, a BET analysis was conducted. Fig. 7(a) presents the isotherm plot for nitrogen adsorption/desorption of LiFePO_4 and $\text{LiFePO}_4/\text{VFLG}$ composites. It can be observed that the two LiFePO_4 and $\text{LiFePO}_4/\text{VFLG}$ composites featured a typical isotherm of type IV, indicating the mesoporous characteristics ($>2\text{ nm}$ and $<50\text{ nm}$) [37], in agreement with FESEM results (Fig. 7). The surface areas of LiFePO_4 and $\text{LiFePO}_4/\text{VFLG}$ composites were measured by multi-point BET and listed in Table 2. The measured BET surface areas of LiFePO_4 and $\text{LiFePO}_4/\text{VFLG}$ composites were $\sim 36,42\text{ m}^2/\text{g}$ and $\sim 43,39\text{ m}^2/\text{g}$, or increased by 19.1% after the addition of graphene, indicating that the presence of graphene increased the surface area of $\text{LiFePO}_4/\text{VFLG}$ composites effectively. This is probably due to the high specific surface area of graphene ($\sim 2630\text{ m}^2/\text{g}$) and the ability to bridge separated or isolated LiFePO_4 particles, forming a conducting network that can effectively reduce the

phenomenon of particle agglomeration [13,32]. According to Kuo et al. [38], graphene sheets can function as a robust scaffold to prevent particle agglomeration. It has been reported that a large surface area can enhance the electrode/electrolyte interface (providing more active sites for electrochemical reactions) and enrich the diffusion pathway for Li^+ ions and electrons, improving the specific capacity and performance of the LIB battery [39].

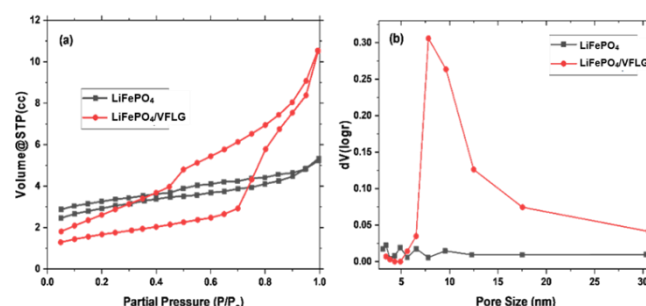


Fig. 7. (a) Nitrogen adsorption/desorption isotherm curve, and (b) Pore distribution curve of LiFePO_4 and LiFePO_4/G

Fig. 7(b) presents the BJH pore size distribution curves of LiFePO_4 and $\text{LiFePO}_4/\text{VFLG}$ composites. It was found that the incorporation of graphene provided a wide distribution of mesopores ($3\text{ nm} - 30\text{ nm}$). Du et al. [39] explained that the presence of mesopores in the LiFePO_4 structure is beneficial to reduce the volume and structure changes and to maintain electrode stability during the electrochemical cycles in LIB application. Furthermore, Table 2 lists the pore diameter and pore volume of LiFePO_4 and $\text{LiFePO}_4/\text{VFLG}$ composites. As seen in Table 2, the pore diameter and pore volume of LiFePO_4 increased by 128.7% and 656.3%, respectively, after the addition of graphene. The significant increase in pore diameter and volume was likely related to graphene, whose flexible structure and high surface area assist in creating more void space within the composite. This is reflected in the research by Weng et al. [40], showing that the addition of graphene can increase the specific surface area and pore volume of the $\text{LiFePO}_4/\text{graphene}$ composite [40]. The bridging of graphene nanosheets and the creation of interconnected conduction networks through cross-linking between adjacent crystallites promote the formation of mesoporous structures, which ultimately increases pore diameter and volume [41]. As shown in the previous TEM analysis section, graphene can limit the growth of LiFePO_4 particles, keeping these particles small and well-dispersed. This results in a growth of the effective surface area and creates more space between particles, thereby increasing the pore volume of the composite. Research indicated that $\text{LiFePO}_4/\text{graphene}$ composites with well-dispersed graphene exhibited an improved electrode performance in LIB applications due to better particle distribution and increased pore size [42].

Table 2. Values of pore diameter, pore volume, and surface area of LiFePO_4 and $\text{LiFePO}_4/\text{Graphene}$ composites

Samples	Pore Diameter, nm (BJH adsorption)	Pore Volume, cc/g (BJH adsorption)	Surface area, m^2/g (Multi-point BET)
LiFePO_4	3.413	0.016	36.418
LiFePO_4/G	7.804	0.121	43.384

4. Conclusion

LiFePO₄/VFLG composites were successfully generated through the sol-gel route. TGA-DSC curves suggested that the integration of graphene strengthen the thermal stability of the LiFePO₄/VFLG composite by inhibiting oxygen diffusion on the LiFePO₄ surface. This was confirmed by the lower mass loss of LiFePO₄/VFLG compared to LiFePO₄ in the TGA curve, as well as the shift of the exothermic peak towards higher temperatures (an increase of 0.15%) in the DSC curve. FESEM-EDX analysis confirmed the presence of graphene, which was homogeneously distributed in the composites. Meanwhile, TEM results revealed that the average particle sizes of LiFePO₄ and LiFePO₄/VFLG composites were 95.98 nm and 75.60 nm, respectively. TEM and HRTEM results furthermore confirmed that graphene intimately contacted LiFePO₄ particles via plane-to-point contact, contributing to the control and reduction of particle size. Physisorption analysis revealed the surface areas of LiFePO₄ and LiFePO₄/VFLG composites at ~36.42 m²/g and ~43.39 m²/g, respectively, representing an increase of 19.1% after the addition of graphene. The incorporation of graphene provided a wider distribution of mesopores (3 nm – 30 nm) compared to bare LiFePO₄. The pore diameter and pore volume of LiFePO₄ increased by 128.7% and 656.3%, respectively after the addition of VFLG. These significant increases were related to the flexibility and high surface area properties of graphene, as well as its ability to limit the growth of LiFePO₄ particles. These excellent physicochemical properties of LiFePO₄/VFLG composites provided a more conducive site for advancing the electrochemical capabilities of LiFePO₄ cathode-based LIB.

Acknowledgements

This work was supported by Badan Riset dan Inovasi Nasional (BRIN) and Lembaga Pengelola Dana Pendidikan (LPDP) Republic of Indonesia via the RIIM research grant (Contract number: 7672/UN19.5.1.3/AL.04/2023).

References

1. Y. Wang, B. Tang, M. Shen, Y. Wu, S. Qu, Y. Hu, Y. Feng, *Environmental impact assessment of second life and recycling for LiFePO₄ power batteries in China*, J. Environ. Manage. 314 (2022) 115083.
2. J. Kumar, R.R. Neiber, J. Park, R.A. Soomro, G.W. Greene, S.A. Mazari, H.Y. Seo, J.H. Lee, M. Shon, D.W. Chang, *Recent progress in sustainable recycling of LiFePO₄-type lithium-ion batteries: Strategies for highly selective lithium recovery*, Chem. Eng. J. 431 (2022) 133993.
3. S.P. Chen, D. Lv, J. Chen, Y.-H. Zhang, F.-N. Shi, *Review on defects and modification methods of LiFePO₄ cathode material for lithium-ion batteries*, Energy & Fuels. 36 (2022) 1232–1251.
4. S. Kaushik, T. Mehta, P. Chand, S. Sharma, G. Kumar, *Recent advancements in cathode materials for high-performance Li-ion batteries: Progress and prospects*, J. Energy Storage. 97 (2024) 112818.
5. Z. Qi, H. Wang, *Advanced thin film cathodes for lithium ion batteries*, Research. 2020 (2020) 2969510.
6. M.A.M.M. Al-Samet, E. Burgaz, *Improving the lithium-ion diffusion and electrical conductivity of LiFePO₄ cathode material by doping magnesium and multi-walled carbon nanotubes*, J. Alloys. Compd. 947 (2023) 169680.
7. R. Tian, H. Liu, Y. Jiang, J. Chen, X. Tan, G. Liu, L. Zhang, X. Gu, Y. Guo, H. Wang, *Drastically enhanced high-rate performance of carbon-coated LiFePO₄ nanorods using a green chemical vapor deposition (CVD) method for lithium ion battery: a selective carbon coating process*, ACS Appl. Mater. Interfaces. 7 (2015) 11377–11386.
8. J. Geng, S. Zhang, X. Hu, W. Ling, X. Peng, S. Zhong, F. Liang, Z. Zou, *A review of graphene-decorated LiFePO₄ cathode materials for lithium-ion batteries*, Ionics. 28 (2022) 4899–4922.
9. A. Amri, Y.B. Hendri, E. Taer, S. Saputro, Y.D.S. Pambudi, Z.T. Jiang, *Novel LiFePO₄/very-few-layer-graphene (LFP/VFLG) composites to improve structural and electrochemical properties of lithium-ion battery cathode*, Ceram Int. 50 (2024) 19806–19813.
10. U. Chasanah, W. Trisunaryanti, Triyono, H.S. Oktaviano, I. Santoso, D.A. Fatmawati, *Study of green reductant effects of highly reduced graphene oxide production and their characteristics*, Commun. Sci. Technol. 7 (2022) 103–111.
11. E. A. Odja, I. Raya, Maming, M. Zakir, A. Karim, D. N. Basir, *Characterization and electrochemical properties analysis of reduced graphene oxide from corn cob carbon as an electrode candidate: Synthesized using modified Hummers method*, Commun. Sci. Technol. 9 (2024) 25–29.
12. L. Kong, Y. Li, W. Feng, *Strategies to solve lithium battery thermal runaway: from mechanism to modification*, Electrochem. Energy Rev. 4 (2021) 633–679.
13. X. Wang, Z. Feng, J. Huang, W. Deng, X. Li, H. Zhang, Z. Wen, *Graphene-decorated carbon-coated LiFePO₄ nanospheres as a high-performance cathode material for lithium-ion batteries*, Carbon N Y. 127 (2018) 149–157.
14. Y. Fu, Q. Wei, G. Zhang, Y. Zhong, N. Moghimian, X. Tong, S. Sun, *LiFePO₄-graphene composites as high-performance cathodes for lithium-ion batteries: The impact of size and morphology of graphene*, Materials. 12 (2019) 842.
15. X. Zhou, F. Wang, Y. Zhu, Z. Liu, *Graphene modified LiFePO₄ cathode materials for high power lithium ion batteries*, J. Mater. Chem. 21 (2011) 3353–3358.
16. T. Liu, S. Sun, Z. Zang, X. Li, X. Sun, F. Cao, J. Wu, *Effects of graphene with different sizes as conductive additives on the electrochemical performance of a LiFePO₄ cathode*, RSC Adv. 7 (2017) 20882–20887.
17. Y. Fu, Q. Wei, G. Zhang, Y. Zhong, N. Moghimian, X. Tong, S. Sun, *LiFePO₄-graphene composites as high-performance cathodes for lithium-ion batteries: The impact of size and morphology of graphene*, Materials. 12 (2019) 842.
18. K.R. Paton, E. Varrla, C. Backes, R.J. Smith, U. Khan, A. O'Neill, C. Boland, M. Lotya, O.M. Istrate, P. King, T. Higgins, S. Barwich, P. May, P. Puczkarski, I. Ahmed, M. Moebius, H. Pettersson, E. Long, J. Coelho, S.E. O'Brien, E.K. McGuire, B.M. Sanchez, G.S. Duesberg, N. McEvoy, T.J. Pennycook, C. Downing, A. Crossley, V. Nicolosi, J.N. Coleman, *Scalable production of large quantities of defect-free few-layer graphene by shear exfoliation in liquids*, Nat. Mater. 13 (2014) 624–630.
19. E. Varrla, K.R. Paton, C. Backes, A. Harvey, R.J. Smith, J. McCauley, J.N. Coleman, *Turbulence-assisted shear exfoliation of graphene using household detergent and a kitchen blender*, Nanoscale. 6 (2014) 11810–11819.
20. A. Amri, Y. Bertilsya Hendri, C.Y. Yin, M. Mahbubur Rahman, M. Altarawneh, Z.T. Jiang, *Very-few-layer graphene obtained from facile two-step shear exfoliation in aqueous solution*, Chem. Eng. Sci. 245 (2021) 116848.
21. Z. J. Fan, J. Yan, T. Wei, G. Q. Ning, L. J. Zhi, J. C. Liu, D. X. Cao, G. L. Wang, F. Wei, *Nanographene-constructed carbon nanofibers grown on*

- graphene sheets by chemical vapor deposition: high-performance anode materials for lithium ion batteries, *ACS Nano*. 5 (2011) 2787–2794.
22. H. Tian, X. Zhao, J. Zhang, M. Li, H. Lu, *LiFePO₄ anchored on pristine graphene for ultrafast lithium battery*, *ACS Appl. Energy Mater.* 1 (2018) 3497–3504.
 23. R. Vinoth, P. Karthik, C. Muthamizhchelvan, B. Neppolian, M. Ashokkumar, *Carrier separation and charge transport characteristics of reduced graphene oxide supported visible-light active photocatalysts*, *Phys. Chem. Chem. Phys.* 18 (2016) 5179–5191.
 24. J. Wang, Z. Shen, M. Yi, *Liquid-exfoliated graphene as highly efficient conductive additives for cathodes in lithium ion batteries*, *Carbon N Y.* 153 (2019) 156–163.
 25. I. Belharouak, C. Johnson, K. Amine, *Synthesis and electrochemical analysis of vapor-deposited carbon-coated LiFePO₄*, *Electrochem. Commun.* 7 (2005) 983–988.
 26. S.R. Das, Q. Nian, M. Saei, S. Jin, D. Back, P. Kumar, D.B. Janes, M.A. Alam, G.J. Cheng, *Single-layer graphene as a barrier layer for intense UV laser-induced damages for silver nanowire network*, *ACS Nano*. 9 (2015) 11121–11133.
 27. W. Wei, W. Lv, M. B. Wu, F. Y. Su, Y. B. He, B. Li, F. Kang, Q. H. Yang, *The effect of graphene wrapping on the performance of LiFePO₄ for a lithium ion battery*, *Carbon N Y.* 57 (2013) 530–533.
 28. S. Wang, F. Wang, Z. Chen, T. Li, C. Yao, M. Wang, H. Wang, H. Wu, *First-principles investigation of the electronic and Li-ion diffusion properties of LiFePO₄ by graphene surface modification*, *Mol Phys.* 121 (2023) e2239380.
 29. B. Wen, C. Sun, B. Bai, *Inhibition effect of a non-permeating component on gas permeability of nanoporous graphene membranes*, *Phys. Chem. Chem. Phys.* 17 (2015) 23619–23626.
 30. Y. Hao, M.S. Bharathi, L. Wang, Y. Liu, H. Chen, S. Nie, X. Wang, H. Chou, C. Tan, B. Fallahazad, *The role of surface oxygen in the growth of large single-crystal graphene on copper*, *Science*. 342 (2013) 720–723.
 31. J. Yang, J. Wang, D. Wang, X. Li, D. Geng, G. Liang, M. Gauthier, R. Li, X. Sun, *3D porous LiFePO₄/graphene hybrid cathodes with enhanced performance for Li-ion batteries*, *J. Power Sources*. 208 (2012) 340–344.
 32. H. Bi, F. Huang, Y. Tang, Z. Liu, T. Lin, J. Chen, W. Zhao, *Study of LiFePO₄ cathode modified by graphene sheets for high-performance lithium ion batteries*, *Electrochim. Acta*. 88 (2013) 414–420.
 33. Z. Tian, S. Liu, F. Ye, S. Yao, Z. Zhou, S. Wang, *Synthesis and characterization of LiFePO₄ electrode materials coated by graphene*, *Appl. Surf. Sci.* 305 (2014) 427–432.
 34. R. Dominko, M. Bele, M. Gaberscek, M. Remskar, D. Hanzel, S. Pejovnik, J. Jamnik, *Impact of the carbon coating thickness on the electrochemical performance of LiFePO₄/C composites*, *J. Electrochem. Soc.* 152 (2005) A607.
 35. H. Wang, N. Zhao, C. Shi, C. He, J. Li, E. Liu, *Interface and Doping Effect on the Electrochemical Property of Graphene/LiFePO₄*, *J. Phys. Chem C*. 120 (2016) 17165–17174.
 36. V.H. Nguyen, H.-B. Gu, *LiFePO₄ batteries with enhanced lithium-ion-diffusion ability due to graphene addition*, *J. Appl. Electrochem.* 44 (2014) 1153–1163.
 37. B. Dong, X. Huang, X. Yang, G. Li, L. Xia, G. Chen, *Rapid preparation of high electrochemical performance LiFePO₄/C composite cathode material with an ultrasonic-intensified micro-impinging jetting reactor*, *Ultrason. Sonochem.* 39 (2017) 816–826.
 38. P.-L. Kuo, C.-H. Hsu, H.-T. Chiang, J.-M. Hsu, *High rate performance intensified by nanosized LiFePO₄ combined with three-dimensional graphene networks*, *J. Nanopart. Res.* 15 (2013) 1966.
 39. G. Du, Y. Xi, X. Tian, Y. Zhu, Y. Zhou, C. Deng, H. Zhu, A. Natarajan, *One-step hydrothermal synthesis of 3D porous microspherical LiFePO₄/graphene aerogel composite for lithium-ion batteries*, *Ceram. Int.* 45 (2019) 18247–18254.
 40. S. Weng, T. Huo, K. Liu, J. Zhang, W. Li, *In-situ polymerization of hydroquinone-formaldehyde resin to construct 3D porous composite LiFePO₄/carbon for remarkable performance of lithium-ion batteries*, *J. Alloys Compd.* 818 (2020) 152858.
 41. F. Fathollahi, M. Javanbakht, H. Omidvar, M. Ghaemi, *Improved electrochemical properties of LiFePO₄/graphene cathode nanocomposite prepared by one-step hydrothermal method*, *J. Alloys Compd.* 627 (2015) 146–152.
 42. H. Liu, C. Miao, Y. Meng, Q. Xu, X. Zhang, Z. Tang, *Effect of graphene nanosheets content on the morphology and electrochemical performance of LiFePO₄ particles in lithium ion batteries*, *Electrochim. Acta*. 135 (2014) 311–318.